Acta Crystallographica Section B
Structural Science
ISSN 0108-7681

Water channel structure of bassanite at high air humidity: crystal structure of $CaSO_4 \cdot 0.625H_2O$

Horst Schmidt,* Iris Paschke, Daniela Freyer and Wolfgang Voigt

TU Bergakademie Freiberg, Institute of Inorganic Chemistry, Leipziger Strasse 29, D-09596 Freiberg, Germany

Correspondence e-mail: horst.schmidt@chemie.tu-freiberg.de

Received 31 May 2011
Accepted 10 October 2011

Structure analysis using single-crystal diffraction was carried out as a contribution to the dispute about the nature of the water channel structure of bassanite ($CaSO_4 \cdot 0.5H_2O$). A recent result of Weiss & Bräu (2009) for the crystal structure of bassanite (monoclinic, space group $C2$) at ambient conditions of air humidity was confirmed. In the presence of high relative air humidity the crystal structure of bassanite transformed due to the incorporation of additional water of hydration. The crystal structure of $CaSO_4 \cdot 0.625H_2O$ was solved by single-crystal diffraction at 298 K and 75% relative air humidity. The experimental results provided an insight into both crystal structures. A model explaining the phase transition from $CaSO_4 \cdot 0.625H_2O$ to $CaSO_4 \cdot 0.5H_2O$ was derived. The monoclinic cell setting of $CaSO_4 \cdot 0.5H_2O$ and the trigonal cell setting of $CaSO_4 \cdot 0.625H_2O$ were confirmed by powder diffraction.

1. Introduction

The crystal structures of the phases gypsum ($CaSO_4 \cdot 2H_2O$; Boeyens & Ichharam, 2002; Pedersen & Semmingsen, 1982), bassanite ($CaSO_4 \cdot 0.5H_2O$, calcium sulfate hemihydrate; Bezou *et al.*, 1995; Weiss & Bräu, 2009), soluble anhydrite ($CaSO_4$, AIII; Flörke, 1952) and anhydrite ($CaSO_4$, AII; Kirfel & Will, 1980; Hartman, 1989) are known in the $CaSO_4$–H_2O system under ambient pressure–temperature conditions. The phases have their greatest importance in the building material sector. Industrial production is based on calcination (production of β-hemihydrate) or autoclaving (production of α-hemihydrate) of dihydrate and later re-hydration to different gypsum products. The two forms, α- and β-hemihydrate, differ in their application characteristics because of different crystallinity. α-hemihydrate forms well-shaped prisms or needles, β-hemihydrate forms flaky, unshaped secondary particles down to extremely small sizes. In spite of these differences the crystal structures of α- and β-hemihydrate are considered to be identical due to their similar powder diffraction pattern. Merely a broadening of reflections is typical for β-hemihydrate. This could be the reason for the authors Follner *et al.* (2002), Bushuev & Borisov (1982) and Christensen *et al.* (2010) indicating a crystal structure for β-hemihydrate which is different from that for α-hemihydrate.

The ongoing controversial discussions are related to the correct description of the water channel occupation in the crystal structure of calcium sulfate hemihydrate (Table 1). Monoclinic as well as trigonal space groups were considered for crystal structure solutions. Recently a single-crystal diffraction experiment (Weiss & Bräu, 2009) proved the existence of a monoclinic sixfold twin in the space group $C2$. This space group is in agreement with the result from Rietveld

Table 1
Crystal structures of $CaSO_4{\cdot}0.5H_2O$ and $CaSO_4$-subhydrates ($CaSO_4{\cdot}xH_2O$, $0.5 \leq x \leq 0.8$) given in the literature.

H_2O	Space group	Reference	ICSD collection code	PDF-2 release 2005 No.
0.5	$P3_121$	Gallitelli (1933)	24474	None
0.5	$P\bar{3}m1$	Caspari (1936)	None	None
0.5	None	Weiser & Milligan (1937)	None	None
0.5	*I*2	Gay (1965)	None	None
0.67	*I*2	Bushuev (1982)	20803	47-0964
0.5	$P6_122$	Bushuev & Borisov (1982)	None	45-0848
0.52	Hexagonal	Frik & Kuzel (1982)	None	None
0.48	Orthorhombic	Frik & Kuzel (1982)	None	None
0.8	$P3_121$	Abriel (1983)	37170	76-2312
0.5	*I*2	Kuzel & Hauner (1987)	None	41-0224
0.62	$P3_121$	Kuzel & Hauner (1987)	None	41-0225
0.74	None	Abriel & Reisdorf (1990)	None	None
0.5, 0.6	*I*2, *C*2	Bezou (1990)	69060,1	None, 80-1236
0.53	*I*2	Abriel & Nesper (1993)	73263	81-1848
0.5, 0.583	*I*2, *C*2	Bezou *et al.* (1995)	79528, 79531	83-0439, 83-0440
0.5	*I*2	Ballirano *et al.* (2001)	92947	None
0.5	*C*2	Becker *et al.* (2005)	None	None
0.5	*I*2, $P3_111$	Christensen *et al.* (2008)	159702	None
0.5	*C*2	Weiss & Bräu (2009)	380286	None
0.5	$P3_111$	Christensen *et al.* (2010)	None	None

refinements on synchrotron radiation and neutron diffraction data (space group *I*2; Bezou *et al.*, 1995). Threefold twinning of bassanite crystals has already been observed by Flörke (1952) with optical polarization microscopy and by Abriel & Nesper (1993) using single-crystal diffraction. Monoclinic symmetry is preferred because of weak superstructure reflections among the strong reflections (Ballirano *et al.*, 2001).

Apart from bassanite, the existence of further hydrates with water content slightly in excess of $0.5H_2O$, the so-called $CaSO_4$-subhydrates ($CaSO_4{\cdot}xH_2O$, $0.5<x \leq 0.8$), are discussed (reviewed by Hand, 1997). Investigations by Bezou (1990), Bezou *et al.* (1995), Kuzel & Hauner (1987), Oetzel (1999) and Oetzel *et al.* (2000) describe changes in the powder diffraction pattern dependant on water vapour pressure starting at $\sim 40\%$ relative air humidity (T = 298 K). An increase from monoclinic to trigonal symmetry was observed at $\sim 75\%$ relative air humidity (Kuzel & Hauner, 1987). Water incorporation above $0.5H_2O$ was confirmed by gravimetric methods (Kuzel & Hauner, 1987; Bezou, 1990). The crystal structure of a subhydrate ($CaSO_4{\cdot}0.6H_2O$) was refined (orthorhombic lattice and space group *C*2) on the basis of the crystal structure of bassanite (Bezou *et al.*, 1995).

The single-crystal structure solution of $CaSeO_4{\cdot}0.625H_2O$ (Fritz *et al.*, 2011) demonstrated that water contents higher than $0.5H_2O$ are possible in bassanite analogous structures, although the unit cell of the selenate is 10% larger compared with the sulfate. As a consequence of the smaller unit-cell volume of $CaSO_4{\cdot}0.5H_2O$ the distances between water molecules are short. Therefore, Lager *et al.* (1984) and Weiss & Bräu (2009) doubt the existence of $CaSO_4$-subhydrates with water contents higher than $0.5H_2O$.

While scientific interest concentrates on crystal structures of phases in the $CaSO_4$–H_2O system, technical reasons motivated experiments with respect to the setting behavior of $CaSO_4{\cdot}0.5H_2O$. For the formulation of gypsum products an exact adjustment of the water–solid ratio is required. Therefore, the hydrate water content of the initial phase has to be known and the safe storage conditions of the hemihydrate powder have to be established (Torrance & Darvell, 1990).

The aim of this work was to prove beyond doubt the existence of $CaSO_4$-subhydrates with water content higher than $0.5H_2O$ by single-crystal diffraction structure solution, because up to now the reversible hemihydrate–subhydrate transformation has been observed and discussed only from changes in the powder pattern data. In order to characterize the starting material and to clarify the discussion about the crystal structure of $CaSO_4{\cdot}0.5H_2O$ (Table 1) a re-investigation of the crystal structure was carried out. Single-crystal structure investigations on calcium sulfate hemihydrate at ambient (30–40%) and high relative air humidity (75%) at room temperature (T = 298 ± 2 K) were performed.

2. Experimental

2.1. Re-investigation of the crystal structure of $CaSO_4{\cdot}0.5H_2O$

α-$CaSO_4{\cdot}0.5H_2O$ crystals from KNAUF company were used. Under the microscope needle-shaped crystals with two different sizes of $\sim 0.4 \times 0.08 \times 0.08$ and $0.05 \times 0.02 \times 0.02$ mm^3 are visible. In comparison to *e.g.* gypsum the crystals are less translucent.

Data collection was performed at room temperature with a Bruker X8 kappa diffractometer and an APEXII detector. Indexing, integration and data reduction was carried out by *APEX*2 software (Bruker, 2005). Structure solution and refinement was performed with *SHELXS*97/*SHELXL*97 (Sheldrick, 2008).

2.1.1. Structure solution and refinement. The crystal structure of $CaSO_4{\cdot}0.5H_2O$ was solved and refined in two different ways.

(i) Refinement of the crystal structure in a small trigonal unit cell, $a = b$ and c, as published by Gallitelli (1933), Caspari (1936), Bushuev & Borisov (1982) and Abriel (1983).

(ii) Data integration in a large trigonal unit cell, $2a = 2b$ and $2c$, and refinement of the crystal structure in a monoclinic unit cell using *hklf*5 data of a sixfold twin as described by Weiss & Bräu (2009).

Crystal data and data on the refinement of $CaSO_4{\cdot}0.5H_2O$ (crystal CaS-HH-1) are given in Table 2.[1] The crystal structure could not be refined successfully in the trigonal crystal system [$R_1 > 4\sigma = 0.112$, wR_2(all) = 0.383]. Obviously the crystal is a

[1] Supplementary data for this paper are available from the IUCr electronic archives (Reference: SN5106). Services for accessing these data are described at the back of the journal.

Table 2
Experimental details for the X-ray data collection and crystallographic parameters for the single-crystal structures of the crystals CaS-HH-1 and CaS-HH-2 (T = 298 ± 2 K).

Crystal shape: needle. Experiments were carried out with Mo $K\alpha$ radiation using a Bruker X8 Kappa APEX2 diffractometer. Data collection used ω and φ scans.

	CaS-HH-1		CaS-HH-2	
Relative air humidity	Ambient	Ambient	75%	Ambient
Crystal data				
Chemical formula	$CaSO_4{\cdot}0.5H_2O$	$CaSO_4{\cdot}0.5H_2O$	$CaSO_4{\cdot}0.625H_2O$	$CaSO_4{\cdot}0.5H_2O$
M_r	145.16	145.16	147.40	145.16
Crystal system, space group	Trigonal, $P3_121$	Monoclinic, $C2$	Trigonal, $P3_221$	Monoclinic, $C2$
a, b, c (Å)	6.9344 (1), 6.9344 (1), 6.3383 (2)	17.5180 (8), 6.9291 (1), 12.0344 (2)	13.8690 (4), 13.8690 (4), 12.7189 (1)	17.5180 (8), 6.9291 (1), 12.0344 (2)
α, β, γ (°)	90, 90, 90	90, 133.655 (1), 90	90, 90, 120	90, 133.655 (1), 90
V (Å^3)	263.95	1056.88 (4)	2118.73 (9)	1056.88 (4)
Z	3	12	24	12
μ (mm^{-1})	2.24	2.24	2.24	2.25
Crystal size (mm)	0.45 × 0.1 × 0.1	0.45 × 0.1 × 0.1	0.40 × 0.08 × 0.07	0.40 × 0.08 × 0.07
Data collection				
Absorption correction	–	–	Numerical	–
T_{min}, T_{max}	–	–	0.641, 0.896	–
$2\theta_{max}$ (°)	59.10	56.00	54.98	54.99
No. of measured, independent and observed [$I > 2\sigma(I)$] reflections	4997, 496, 465	4481, 4481, 4071	38 925, 3252, 2578	15 532, 15 543, 12 774
R_{int}	0.020	–	0.043	–
$(\sin\theta/\lambda)_{max}$ (Å^{-1})	0.695	0.662	0.650	0.650
Range of h, k, l	$h = -9 \rightarrow 7$, $k = -8 \rightarrow 9$, $l = -5 \rightarrow 8$	$h = -16 \rightarrow 18$, $k = -7 \rightarrow 7$, $l = -5 \rightarrow 5$	$h = -17 \rightarrow 17$, $k = -17 \rightarrow 17$, $l = -16 \rightarrow 16$	$h = -17 \rightarrow 17$, $k = -7 \rightarrow 8$, $l = -5 \rightarrow 5$
Refinement				
$R_1 > 4\sigma$	0.112	0.046	0.039	0.043
R_1 all	0.115	0.056	0.061	0.058
wR_2 all	0.383	0.120	0.108	0.097
G.O.F.	3.395	1.059	1.029	0.969
No. of reflections	496	4481	3252	15 543
No. of parameters	34	193	258	193
No. of restraints	0	1	5	1
$\Delta\sigma_{max}$, $\Delta\sigma_{min}$ (e Å^{-3})	1.65, −2.23	1.05, −0.65	0.53, −0.45	0.625, −0.48
BASF	–	0.382, 0.237, 0.049 0.036, 0.039	0.0119, 0.825, 0.055	0.309,0.328,0.017 0.027, 0.028

sixfold twin with twin domains in the monoclinic space group $C2$ [$R_1 > 4\sigma = 0.046$, wR_2(all) = 0.120]. This result is coincident with the investigation of Weiss & Bräu (2009).

2.2. Crystal structure of calcium sulfate hemihydrate at high relative air humidity

Crystals of α-$CaSO_4{\cdot}0.5H_2O$ were stored for 2 weeks in a desiccator above saturated sodium chloride solution, which guarantees a relative air humidity of 75.47 ± 0.2% (298 ± 2 K; Greenspan, 1977). One of those crystals (CaS-HH-2) with dimensions similar to those of CaS-HH-1 was enclosed directly in a Hilgenberg glass capillary (diameter 0.3 mm; Fig. 1). In the lower part of the capillary a drop of saturated sodium chloride solution was placed in order to keep the relative air humidity at 75%. The capillary was closed by wax.

2.2.1. Structure solution and refinement. Fig. 2 shows reconstructed reciprocal space planes ($hk0$) and ($hk1$) for diffraction experiments on crystals CaS-HH-1 and CaS-HH-2. Compared with the diffraction pattern of CaS-HH-1 in Fig. 2(*a*), the reciprocal space of CaS-HH-2 at high relative air humidity shows additional reflections in the ($hk0$) plane (Fig. 2*b*). After the opening of the capillary, and thus the decrease of air humidity to ambient conditions, these reflections disappear and the pattern becomes identical to that of CaS-HH-1 (Fig. 2*c*).

The diffraction space of the crystal CaS-HH-2, measured at 75% relative air humidity, was indexed using a trigonal unit cell with a = 13.84 and c = 12.74 Å. A structure solution in the space group $P3_221$ was found by direct methods. The refinement resulted in a sensible structure with some distortions (negative anisotropic displacements). Twinning was indicated by the Flack parameter (Flack, 1983) and the refinement result was improved by the introduction of merohedral twinning ($0\bar{1}0/\bar{1}00/00\bar{1}$), which is common for trigonal crystals. Additionally the crystal is a racemic twin. The positions of H atoms were located from a difference electron density map and during least-squares refinement their distances to O atoms were restrained to 0.82 ± 0.02 Å.

After opening of the capillary the crystal CaS-HH-2 is again monoclinic and twinned analogous to the result for the crystal

CaS-HH-1. The structural changes at high relative air humidity are reversible.

Crystal data and data on the refinement of the sample CaS-HH-2 at the two different humidities are given in Table 2.

2.3. Powder diffraction

Powder diffraction experiments were carried out with a Bruker D5000 Theta/Theta diffractometer (Cu $K\alpha$ radiation, primary and secondary Goebel mirror, scintillation detector) adapted by a temperature-controlled humidity chamber 'TC-Humidity' from MRI company. The α-hemihydrate crystals were powdered and mixed with tungsten as an internal standard. The sample was placed at the sample holder of the humidity chamber for 8 h at 300 K and 75% relative air humidity before measurement was started. (Pre-investigations have shown a slower hydration kinetic of α-hemihydrate than for β-hemihydrate. The reversible transformation of the α-hemihydrate to $CaSO_4{\cdot}0.625H_2O$ needs a few hours. So the time to form the subhydrate from the α-form is sufficient in 3–4 h and guaranteed in 8 h.) The temperature of the sample holder over the total time was stable with 300 $\pm$ 0.2 K, and the uncertainty in relative air humidity amounted to 1%. For the measurement of the α-hemihydrate the relative air humidity was decreased from 75 to 30%. After a holding time of 8 h again at this low air humidity the reconstitution of the α-hemihydrate structure was completed for data collection. The high-resolution X-ray powder diffraction patterns of the two phases were collected in steps of 0.01° 2θ at a scanning time of 30 s per step (58 h total). For the refinement of the lattice parameters obtained by single-crystal structure analysis the program *TOPAS* (Bruker, 2009) was used. Owing to the Goebel mirror optics an empirical parameterization of line profile shapes was carried out from the precise measurement of the NIST line profile standard C79298-A3244-B264 (corundum plate) in the 2θ range 10–80° in the humidity chamber. The zero point error was calibrated using tungsten powder as an internal standard. Third-order Chebychev polynomials were applied for modelling the background. Finally the precise lattice parameters for $CaSO_4{\cdot}0.5H_2O$ and $CaSO_4{\cdot}0.625H_2O$ were determined by a LeBail fit.

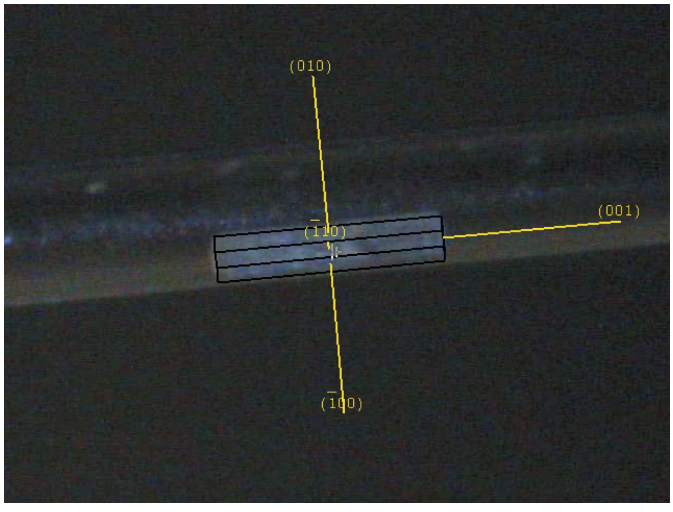

Figure 1
Crystal CaS-HH-2 inside the capillary (diameter 0.3 mm, crystal size 0.4 × 0.08 × 0.07 mm); morphology and crystal size determined by Bruker *APEX*2 scale package (Bruker, 2005).

3. Results and discussion

3.1. Refinement of the lattice parameters

The existence and formation of $CaSO_4$-subhydrates from $CaSO_4$-hemihydrate is discussed in the literature on the basis of powder diffraction experiments only. Structural changes were derived by indexing or Rietveld refinements of the powder pattern data from small changes in reflex positions dependent on the relative air humidity. As a result many stoichiometries ($CaSO_4{\cdot}xH_2O$, $0.5 \leq \times \leq 0.8$) are given in the literature (Table 1).

Furthermore, a discussion on the best description of the crystal structure of $CaSO_4{\cdot}0.5H_2O$ is mainly caused by the trigonal single-crystal diffraction pattern (Fig. 2). In the case of a trigonal diffraction pattern it is often not easy to decide whether the crystal is trigonal or monoclinic and threefold twinned. In order to validate the monoclinic cell setting of

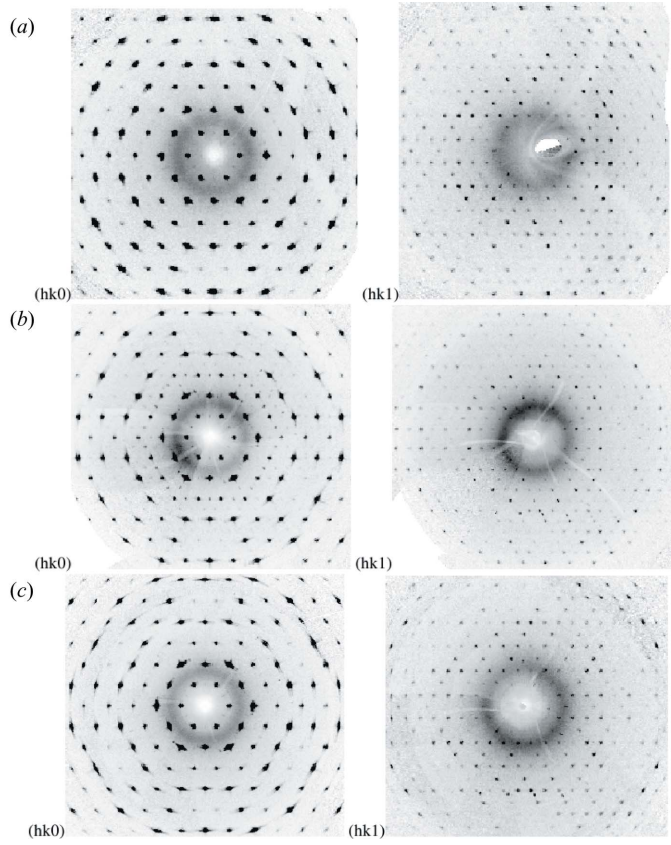

Figure 2
Reconstructed reciprocal space planes of (*a*) $CaSO_4{\cdot}0.5H_2O$ (crystal CaS-HH-1), (*b*) $CaSO_4{\cdot}0.625H_2O$ (crystal CaS-HH-2 in the capillary above saturated sodium chloride solution at 298 $\pm$ 2 K and 75% relative air humidity) and (*c*) $CaSO_4{\cdot}0.5H_2O$ (crystal CaS-HH-2 after opening of the capillary).

$CaSO_4{\cdot}0.5H_2O$ and the trigonal cell setting of $CaSO_4{\cdot}0.625H_2O$ against a bulk of crystals, refinement of the lattice parameters by additional powder diffraction experiments was carried out under appropriate conditions.

Refinement of the lattice parameters of the hemihydrate resulted in the values: a = 17.5180 (8), b = 6.9291 (1), c = 12.0344 (2) Å, β = 133.655 (1)° and V = 1056.88 (4) Å^3 (reliability factors for all reflections: R_{wp} = 0.140, R_p = 0.088, GOF = 1.52). Refinement of the lattice parameters of $CaSO_4{\cdot}0.625H_2O$ resulted in the values $a = b$ = 13.8690 (4), c = 12.7189 (1) Å and V = 2118.73 (9) Å^3 (reliability factors for all reflections: R_{wp} = 0.146, R_p = 0.095 and GOF = 1.47). The diffraction pattern of the hemihydrate ($CaSO_4{\cdot}0.5H_2O$) and the subhydrate ($CaSO_4{\cdot}0.625H_2O$), measured for refinement, as well as the best LeBail fit of the profile and the difference curve between both are shown in Figs. 3 and 4.

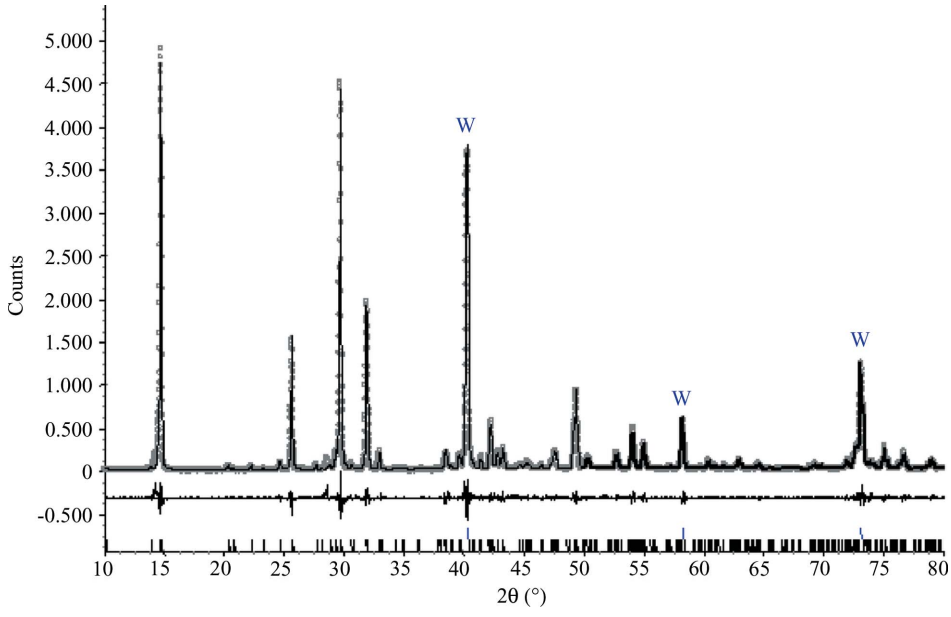

Figure 3
X-ray powder pattern of hemihydrate ($CaSO_4{\cdot}0.5H_2O$) at 300 K and 30% relative air humidity with tungsten (W) as an internal standard [observed pattern (circles), the best LeBail fit profiles (line), and the difference curve between the observed and the calculated profiles (below)].

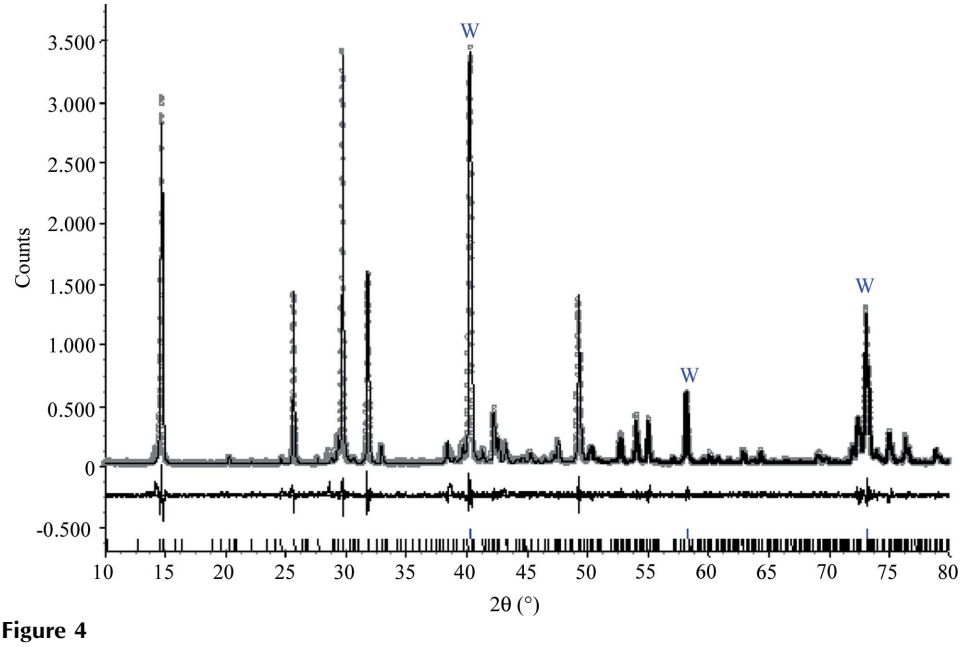

Figure 4
X-ray powder pattern of the subhydrate ($CaSO_4{\cdot}0.625H_2O$) at 300 K and 75% relative air humidity with tungsten (W) as an internal standard [observed pattern (circles), the best LeBail fit profiles (line), and the difference curve between the observed and the calculated profiles (below)].

3.1.1. Comparison with literature results. The observed powder patterns of $CaSO_4{\cdot}0.625H_2O$ and the reference lines of $CaSO_4{\cdot}0.583H_2O$ (PDF: 083-0440; Bezou *et al.*, 1995) and $CaSO_4{\cdot}0.62H_2O$ (PDF: 41-0225; Kuzel & Hauner, 1987) show good agreement. Kuzel & Hauner (1987) determined a trigonal unit cell (a = 13.8615, c = 12.7391 Å), but no structure solution was performed. The unit cell chosen by Bezou *et al.* (1995) (a = 11.9845, b = 6.9292, c = 12.7505 Å and β = 90°) has been obtained by Rietveld refinement based on the monoclinic hemihydrate structure. From this refinement the slight shifts and splitting of some reflections could be described quite well compared with the detailed pattern in Fig. 5. The correct large trigonal unit cell was also considered by Bezou *et al.* (1995), but discarded by the authors owing to statistical reasons. However, the structural changes of the hemihydrate–subhydrate conversion can be observed by powder patterns and are now referenced by the correct crystal structure of $CaSO_4{\cdot}0.625H_2O$, formed at ambient temperature and 75% relative air humidity.

3.2. Comparison of the crystal structures of $CaSO_4{\cdot}0.5H_2O$ and $CaSO_4{\cdot}0.625H_2O$

3.2.1. Description of the crystal structures. The crystal structures of $CaSO_4{\cdot}0.5H_2O$ and $CaSO_4{\cdot}0.625H_2O$ differ mainly in the positions of water molecules. The crystal structures consist of Ca–SO_4 chains, which form channels perpendicular to the projection plane in Fig. 6. The diameter of the channels allows the inclusion of H_2O molecules. The H_2O

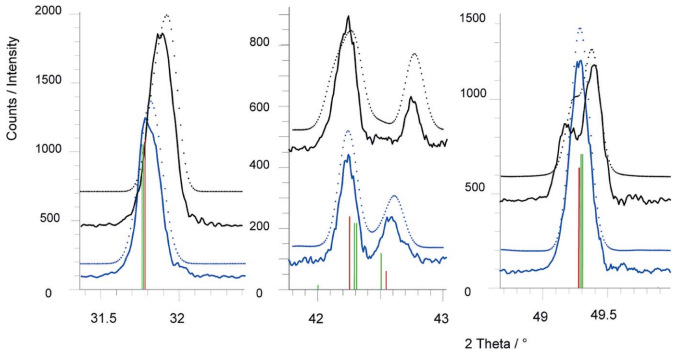

Figure 5
Details of the powder pattern observed for $CaSO_4{\cdot}0.5H_2O$ (black line: observed; dotted: Le Bail fit profile) and $CaSO_4{\cdot}0.625H_2O$ (blue line: observed; dotted: Le Bail fit profile) compared with the reference data of $CaSO_4{\cdot}0.62H_2O$ (brown lines; PDF: 41-0225; Kuzel & Hauner, 1987) and $CaSO_4{\cdot}0.583H_2O$ (green lines; PDF: 083-0440; Bezou *et al.*, 1995).

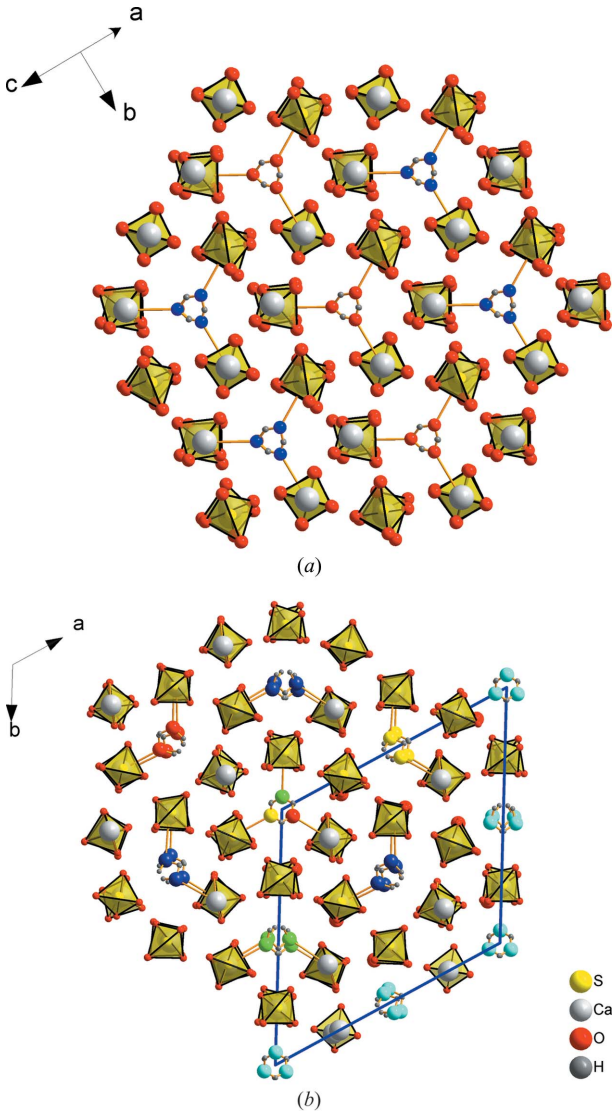

Figure 6
Crystal structures of (*a*) $CaSO_4{\cdot}0.5H_2O$, viewing direction (100), and (*b*) $CaSO_4{\cdot}0.625H_2O$, viewing direction (001). Water O atoms are red, blue, green and yellow in order to indicate different relative height positions of the water molecules. Crystal structure pictures were created with *DIAMOND* (Brandenburg, 2006).

molecules belong to the coordination sphere of Ca^{2+}. The arrangement of water inside the channels of $CaSO_4{\cdot}0.5H_2O$ is identical for all channels.

$CaSO_4{\cdot}0.625H_2O$ forms a complex pattern of water channels. From the *c* axis projection in Fig. 6(*b*) four different water channels are apparent. This symmetric arrangement of water channels is caused by the inclusion of one additional water molecule in three of four channels. The inclusion of an additional water molecule is accompanied by the positional change of a second water molecule.

In $CaSO_4{\cdot}0.5H_2O$ some water channels are shifted by half of the lattice translation vector (Fig. 7*a*). Therefore, the lattice of the crystal structure is C-centered (space group *C*2).

From Fig. 7(*b*) it is obvious that in the crystal structure of $CaSO_4{\cdot}0.625H_2O$ three water channels are systematically translated against each other. A fourth, unchanged channel exists compared with $CaSO_4{\cdot}0.5H_2O$.

3.2.2. Explanation of the crystal structures. In both compounds eight sulfate O atoms form the coordination polyhedron of Ca^{2+} given in Fig. 8(*a*). The Ca–O polyhedron is

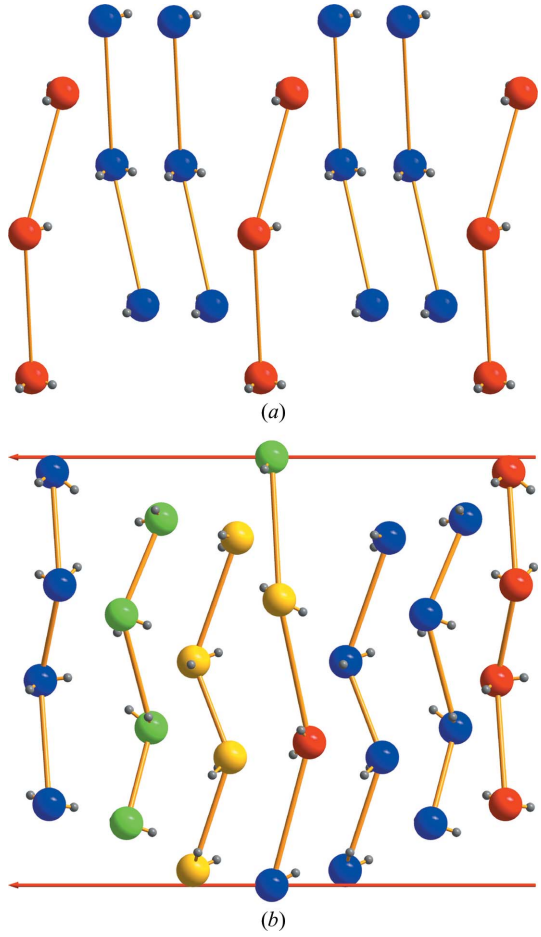

Figure 7
Water channel structures of (*a*) $CaSO_4{\cdot}0.5H_2O$, viewing direction $(\bar{1}0,1,10)$, and (*b*) $CaSO_4{\cdot}0.625H_2O$, viewing direction $(\bar{3}10)$. Ca ions and SO_4 groups are omitted. Different colors of O atoms indicate the different relative positions of the water molecules. In (*b*) these water molecules are systematically shifted compared with the water positions of the unchanged channel in the middle of the picture.

asymmetric and possesses an angular and a planar side. Therefore, the channels are convenient for the inclusion of water. While O atoms coordinate on the flat side to Ca^{2+}, H atoms bond on the angular side and consequently a charge balance is reached. Inside a channel angular and planar sides of Ca–O polyhedra alternate (Fig. 8*b*).

In Figs. 9–12 the Ca—O connectivity (*a*) and hydrogen bonds to the Ca–SO_4 chains (*b*) of two adjacent channels are illustrated. In the case of $CaSO_4{\cdot}0.5H_2O$ a shift of water positions by 0.5 of the lattice translation vector (Fig. 9) and adjacent channels of the same height (Fig. 10) are observable. If the heights of adjacent channels are identical, hydrogen bonds connect at the same height from both channels to the edges of the SO_4 tetrahedra. As a channel cannot be translated by 0.5 with respect to two channels, which are also adjacent and shifted by 0.5 against each other, adjacent channels of the same height have to exist.

Regarding the crystal structure of $CaSO_4{\cdot}0.625H_2O$, two adjacent channels occupied by four water molecules per lattice translation are given in Fig. 11. The connectivity of water molecules to the Ca–SO_4 chains follows the principle

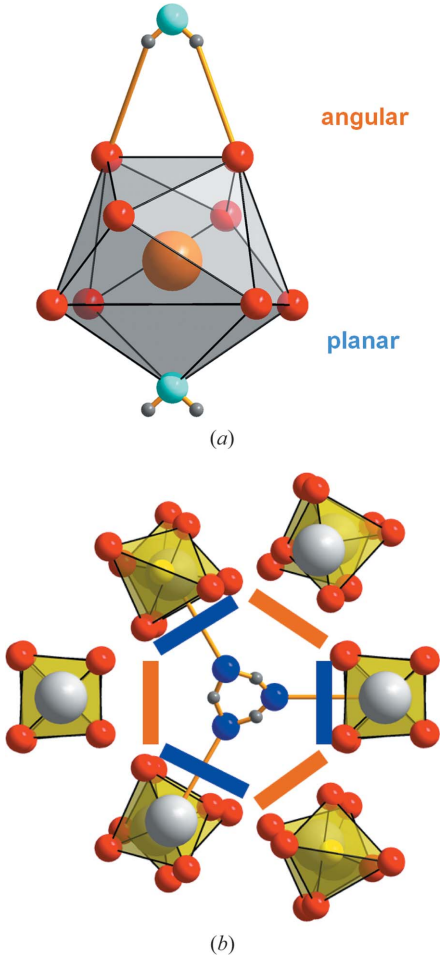

Figure 8
Ca—O coordination polyhedron in $CaSO_4$-hemihydrate as well as in $CaSO_4$-subhydrate. (*a*) Asymmetry of the polyhedron; (*b*) alignment of angular and planar sides in the channel.

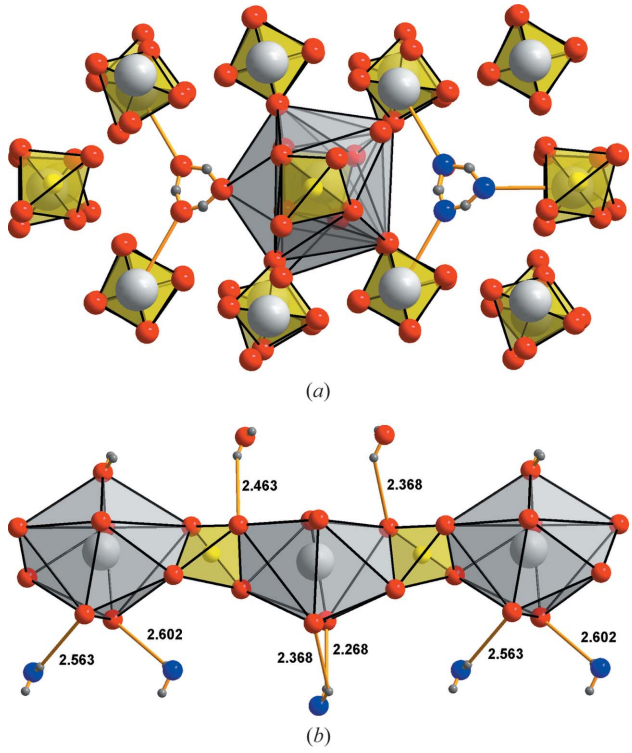

Figure 9
Adjacent channels in the crystal structure of $CaSO_4{\cdot}0.5H_2O$ with different heights. (*a*) H_2O—Ca bonding; (*b*) hydrogen bonding to the Ca–SO_4 chains. Bond lengths are given in Å. Colors of water O atoms are chosen in accordance with Fig. 6.

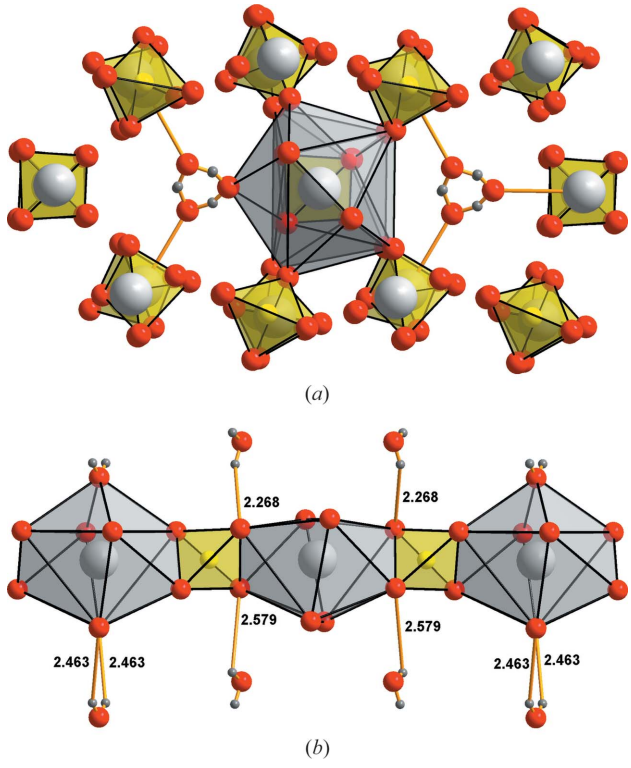

Figure 10
Adjacent channels in the crystal structure of $CaSO_4{\cdot}0.5H_2O$ with the same height. (*a*) H_2O–Ca bonding; (*b*) hydrogen bonding to the Ca–SO_4 chains. Bond lengths are given in Å. Colors of water O atoms are chosen in accordance with Fig. 6.

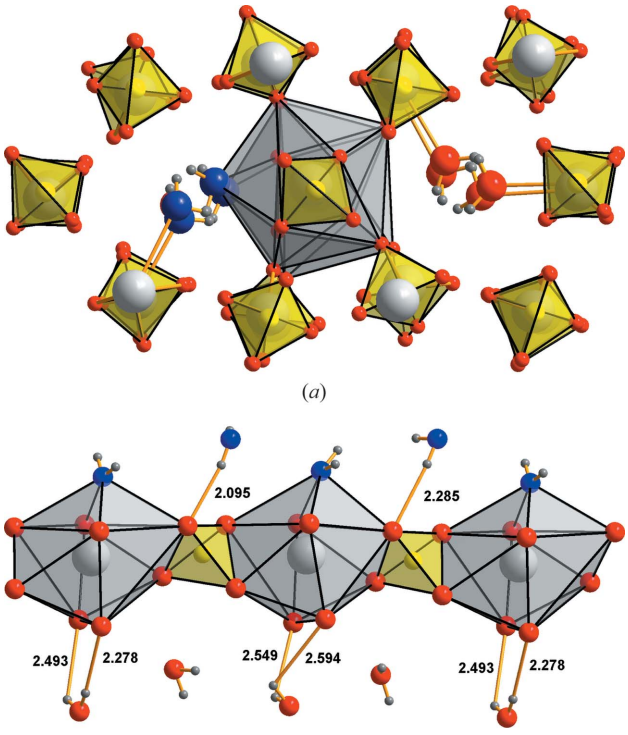

Figure 11
Adjacent channels in the crystal structure of $CaSO_4{\cdot}0.625H_2O$. (*a*) H_2O–Ca bonding; (*b*) hydrogen bonding to the Ca–SO_4 chains. Bond lengths are given in Å. Colors of water O atoms are chosen in accordance with Fig. 6.

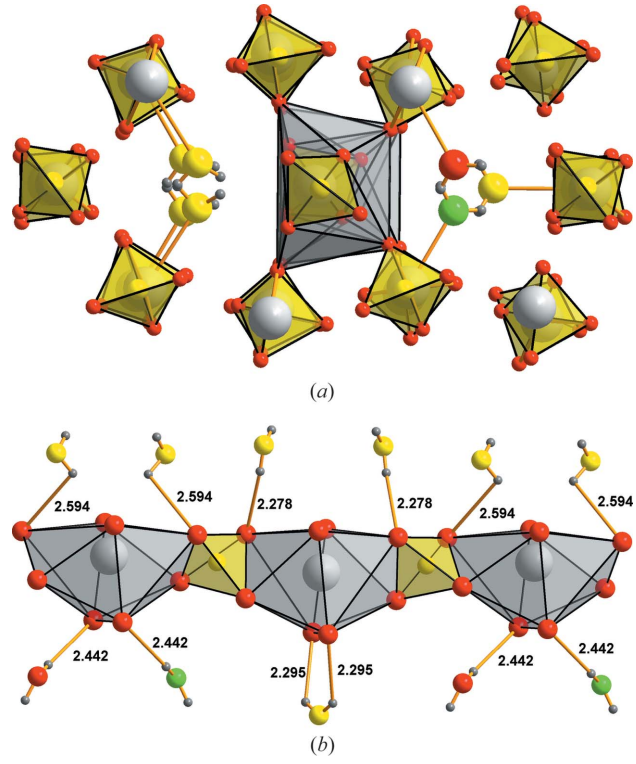

Figure 12
Adjacent channels in the crystal structure of $CaSO_4{\cdot}0.625H_2O$. (*a*) H_2O–Ca bonding; (*b*) hydrogen bonding to the Ca–SO_4 chains. Bond lengths are given in Å. Colors of water O atoms are chosen in accordance with Fig. 6.

described above. O atoms bond on the flat side of the Ca–O polyhedron to Ca^{2+} and hydrogen bonds are formed on the angular side. If a water O atom bonds on the flat side of each Ca–O polyhedron of a Ca–SO_4 chain, the additional negative charge is equalized by hydrogen bonds on the angular side.

A channel occupied by three water molecules exists because an additional channel with four water molecules does not follow the observed principle of H_2O–Ca–H_2O connectivity. The compensation of the negative charge caused by water O atoms bonded to each Ca^{2+} of a Ca–SO_4 chain is geometrically impossible.

The channel occupied by three water molecules, indicated by differently colored water O atoms in Figs. 6, 7 and 12, is stabilized by a shift of water molecules relative to the channel containing four water molecules. Consequently, hydrogen bonds originating from adjacent channels do not connect to the same SO_4 tetrahedron.

3.3. Phase transition

Starting from high relative air humidity conditions $CaSO_4{\cdot}0.625H_2O$ transforms from a crystal structure in the space group $P3_221$ to $CaSO_4{\cdot}0.5H_2O$ in the space group $C2$ accompanied by threefold twinning. The reason for symmetry reduction at lower air humidity associated with lower water content is given by the existence of water channels of identical height, which were discussed before according to Fig. 10. Hydrogen bonds of water molecules of adjacent channels connect to identical SO_4 tetrahedra and repulsion occurs. Hence a slight prolongation of the Ca—O bond in this direction is observable ('stretching' in Fig. 13). The prolongation of the Ca—O bonds in one direction leads to the formation of forces induced by internal strain. In order to avoid mechanical stress the structure is tilted perpendicular to the driving force and becomes monoclinic (Fig. 13).

The group–subgroup relationship is of a common type (Wondratschek & Müller, 2006) and $C2$ is a maximal translationengleiche subgroup of $P3_221$ (Fig. 14). However, no

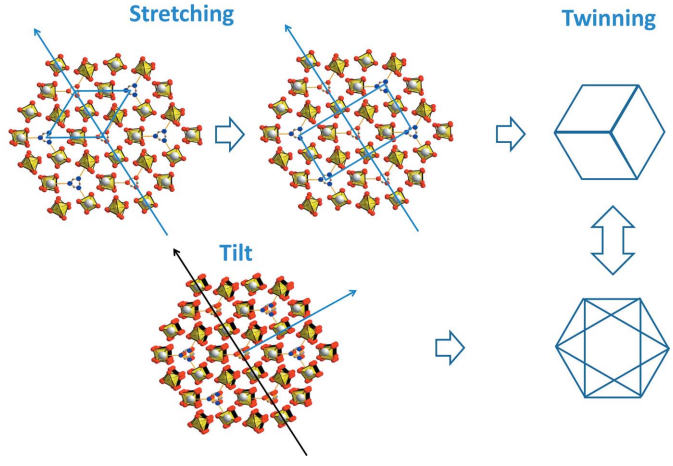

Figure 13
Formation and twinning of $CaSO_4{\cdot}0.5H_2O$, *e.g.* the transformation from $CaSO_4{\cdot}0.625H_2O$.

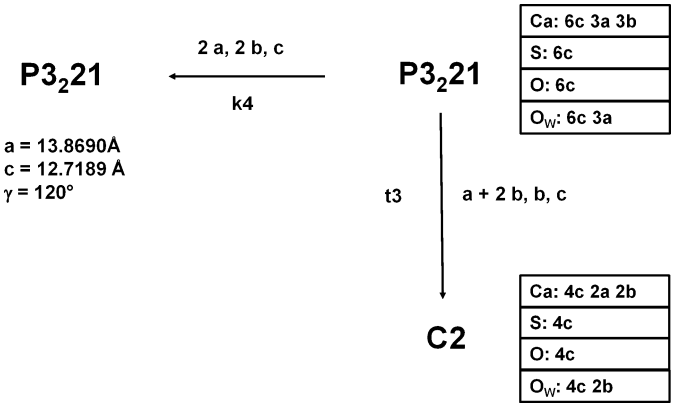

Figure 14
Bärnighausen diagram (Bärnighausen, 1980) of the $CaSO_4{\cdot}0.625H_2O$–$CaSO_4{\cdot}0.5H_2O$ transition.

transition path was found. The unit cell of the high-symmetry crystal structure is larger as a consequence of water incorporation. Therefore, for comparison of relations between structure types a trigonal crystal structure with a smaller *a*/2, *b*/2, *c* unit cell must be considered. The crystal structure in this unit cell is a klassengleiche supergroup with index 4. Owing to continuous loss of water a second-order phase transition occurs. The translationengleiche transformation from space group $P3_221$ to space group $C2$ with index 3 leads to the formation of a threefold twin (Fig. 13). With respect to the present experimental results the twinned trigonal crystal is transformed to a sixfold twinned monoclinic crystal (three large and three small domains; see BASF twin fractions in Table 2).

4. Conclusion

The crystal structure of $CaSO_4{\cdot}0.5H_2O$ was reinvestigated by single-crystal diffraction. The solution of Weiss & Bräu (2009) in the space group $C2$ was confirmed. In the presence of increased relative air humidity of 75% and 298 ± 2 K a transformed bassanite phase was found. The crystal structure of $CaSO_4{\cdot}0.625H_2O$ was solved by single-crystal diffraction for the first time. The lattice parameters of this $CaSO_4$-subhydrate as well as of $CaSO_4{\cdot}0.5H_2O$ were refined by powder diffraction and consequently the cell setting of both compounds was confirmed.

Thus, the hydrate water content of bassanite, $CaSO_4{\cdot}0.5H_2O$, the most important gypsum building material, depends on temperature and relative air humidity. At ambient conditions (room temperature and $\sim 40\%$ relative air humidity) the well known bassanite stoichiometry $CaSO_4{\cdot}0.5H_2O$ becomes evident. By increasing the relative air humidity additional water of crystallization is incorporated.

The crystal structures of $CaSO_4{\cdot}0.5H_2O$ and $CaSO_4{\cdot}0.625H_2O$ were compared with respect to their water channel structure. The water is bonded to Ca–O polyhedra in both crystals following the principle of charge balance. While water O atoms bond on the flat sides of the Ca–O polyhedra, the additional negative charge is equalized by hydrogen bonds on the angular sides of Ca—O polyhedra. In the crystal structure of $CaSO_4{\cdot}0.625H_2O$ all adjacent water channels are shifted against each other. However, in the crystal structure of $CaSO_4{\cdot}0.5H_2O$ adjacent water channels of identical height exist. This fact in particular is responsible for the lower symmetry of $CaSO_4{\cdot}0.5H_2O$.

References

Abriel, W. (1983). *Acta Cryst.* C**39**, 956–958.
Abriel, W. & Nesper, R. (1993). *Z. Kristallogr.* **205**, 99–113.
Abriel, W. & Reisdorf, K. (1990). *J. Solid State Chem.* **85**, 23–30.
Ballirano, P., Maras, A., Meloni, S. & Caminiti, R. (2001). *Eur. J. Mineral.* **13**, 985–993.
Bärnighausen, H. (1980). *Commun. Math. Chem.* **9**, 139–175.
Becker, A., Sotje, I., Paulmann, C., Beckmann, F., Donath, T., Boese, R., Prymak, O., Tiemann, H. & Epple, M. (2005). *Dalton Trans.* **10**, 1545–1550.
Bezou, C. (1990). *C. R. Acad. Sci. Paris Ser. II*, **311**, 1493–1498.
Bezou, C., Nonat, A., Mutin, J. C., Christensen, A. N. & Lehmann, M. S. (1995). *J. Solid State Chem.* **117**, 165–176.
Boeyens, J. C. A. & Ichharam, V. V. H. (2002). *Z. Kristallogr. New Cryst. Struct.* **217**, 9–10.
Brandenburg, K. (2006). *DIAMOND*. Crystal Impact GbR, Bonn, Germany.
Bruker (2005). *APEX*2. Bruker AXS Inc., Madison, Wisconsin, USA.
Bruker (2009). *TOPAS*, Version 4.2. Bruker AXS Inc., Madison, Wisconsin, USA.
Bushuev, N. N. (1982). *Russ. J. Inorg. Chem.* **27**, 344–347.
Bushuev, N. N. & Borisov, V. M. (1982). *Russ. J. Inorg. Chem.* **27**, 341–344.
Caspari, W. A. (1936). *Proc. R. Soc. London Ser. A*, **155**, 41–48.
Christensen, A. N., Jensen, T. R. & Nonat, A. (2010). *Dalton Trans.* **39**, 2044–2048.
Christensen, A. N., Olesen, M., Cerenius, Y. & Jensen, T. R. (2008). *Chem. Mater.* **20**, 2124–2132.
Flack, H. D. (1983). *Acta Cryst.* A**39**, 876–881.
Flörke, O. W. (1952). *Neues Jahrb. Miner. Abh.* **84**, 189–240.
Follner, S., Wolter, A., Preusser, A., Indris, S., Silber, C. & Follner, H. (2002). *Cryst. Res. Technol.* **37**, 1075–1087.
Frik, M. & Kuzel, H. J. (1982). *Fortschr. Mineral*, **60**, 79–80.
Fritz, S., Schmidt, H., Paschke, I., Magdysyuk, O., Dinnebier, R., Freyer, D. & Voigt, W. (2011). *Acta Cryst.* B**67**, 293–301.
Gallitelli, P. (1933). *Period. Mineral.* **4**, 132–171.
Gay, P. (1965). *Mineral. Mag.* **35**, 354–362.
Greenspan, L. (1977). *J. Res. Natl Bur. Stand. A*, **81**, 89–96.
Hand, R. (1997). *Br. Ceram. Trans.* **96**, 116–120.
Hartman, P. (1989). *Eur. J. Mineral.* **1**, 721–722.
Kirfel, A. & Will, G. (1980). *Acta Cryst.* B**36**, 2881–2890.
Kuzel, H. J. & Hauner, M. (1987). *Zement-Kalk-Gips*, **12**, 628–632.
Lager, G. A., Armbruster, T., Rotella, F. J., Jorgensen, J. D. & Hinks, D. G. (1984). *Am. Mineral.* **69**, 910–918.
Oetzel, M. (1999). Thesis. RWTH Aachen.
Oetzel, M., Heger, G. & Koslowski, T. (2000). *Zement-Kalk-Gips*, **6**, 354–361.
Pedersen, B. F. & Semmingsen, D. (1982). *Acta Cryst.* B**38**, 1074–1077.
Sheldrick, G. M. (2008). *Acta Cryst.* A**64**, 112–122.
Torrance, A. & Darvell, B. W. (1990). *Aust. Dent. J.* **35**, 230–235.
Weiser, H. B. & Milligan, W. O. (1937). *J. Am. Chem. Soc.* **59**, 1456–1458.
Weiss, H. & Bräu, M. F. (2009). *Angew. Chem.* **121**, 3572–3576.
Wondratschek, H. & Müller, U. (2006). *International Tables for Crystallography*, Vol. A1. Heidelberg: Springer.